

Constraining three-nucleon forces with multimessenger data

Andrea Maselli,^{1,2,3} Andrea Sabatucci,^{3,4} and Omar Benhar^{4,3}

¹*Gran Sasso Science Institute (GSSI), I-67100 L'Aquila, Italy*

²*INFN, Laboratori Nazionali del Gran Sasso, I-67100 Assergi, Italy*

³*Dipartimento di Fisica, "Sapienza" Università di Roma, Piazzale Aldo Moro 5, 00185, Roma, Italy*

⁴*INFN, Sezione di Roma, Piazzale Aldo Moro 5, 00185, Roma, Italy*

(Dated: May 27, 2021)

We report the results of a study aimed at inferring direct information on the repulsive three-nucleon potential V_{ijk}^R —driving the stiffness of the nuclear matter equation of state at supranuclear densities—from astrophysical observations. Using a Bayesian approach, we exploit the measurements of masses, radii and tidal deformabilities performed by the NICER satellite and the LIGO/Virgo collaboration, as well as the mass of the heaviest observed pulsar, to constrain the strength of V_{ijk}^R . The baseline of our analysis is the widely employed nuclear Hamiltonian comprising the Argonne v_{18} nucleon-nucleon potential and the Urbana IX model of three-nucleon potential. The numerical results, largely determined by the bound on the maximum mass, suggest that existing and future facilities have the potential to provide valuable new insight into microscopic nuclear dynamics at supranuclear densities.

I. INTRODUCTION

Over the past decade, the availability of astrophysical data collected by electromagnetic (EM) observatories [1–9] and gravitational-wave (GW) interferometers [10–12], supplemented by the information obtained from Earth-based laboratory experiments [13–21], has opened a new era for the investigation of neutron star (NS) structure and dynamics.

The studies aimed at constraining the equation of state (EOS) of NS matter have recently benefit from measurements of the tidal deformabilities [22–27]—encoding the footprint of tidal interactions on the signal emitted by a binary system—performed within the GW band. Because the tidal deformability depends on the internal composition of the stars, any information on its value is potentially a source of novel insight into the EOS. The discovery of GW170817 has triggered a large number of efforts aimed at constraining the NS structure, also exploiting multimessenger approaches based on joint GW-EM analyses [28–46]. For extensive reviews on this topic, see Refs. [47, 48] and references therein.

Besides being a valuable source of information on average properties of dense matter embodied in the EOS, as well as on the possible occurrence of a transition to exotic high-density phases—in which constituents other than nucleons are the relevant degrees of freedom—the new data provide an unprecedented opportunity to constrain the existing models of nuclear dynamics at supranuclear density.

The description of nuclear systems in terms of point-like protons and neutrons interacting through phenomenological two- and three-body forces—hereafter Nuclear Many-Body Theory, or NMBT—has proved remarkably successful. The results of calculations based on NMBT account for a variety of observables of nuclei with $A \leq 12$ —including the energies of ground and low-lying excited states and electromagnetic form factors [49]—and provide accurate and reliable estimates of the empirical

equilibrium properties of isospin-symmetric matter [50]. Applications of NMBT in the region of supranuclear densities, however, unavoidably involve a degree of extrapolation.

Phenomenological NN potentials account for scattering data up to large energies—typically ~ 600 MeV in the lab frame, well beyond pion production threshold—as well as for the effects of high-momentum components in the deuteron wave-function. Therefore, these models are expected to be suitable to describe interactions in matter at densities as large as $\sim 4\rho_0$, with ρ_0 being the nuclear matter equilibrium density [51].

Three-nucleon (NNN) potentials, on the other hand, are designed to explain only the ground-state energy of the three-nucleon bound states and nuclear matter equilibrium properties, while being totally unconstrained in the regime corresponding to densities $\rho \gg \rho_0$, in which the contribution of three-nucleon interactions rapidly increases to become dominant. In this article, we report the results of an analysis based on a novel approach, in which astrophysical data are exploited to obtain information on the strength of the repulsive component of the NNN potential, which largely determines the compressibility of matter at supranuclear densities.

It has to be stressed that our approach is conceptually different from the one aimed at constraining the EOS of dense matter, and has a much broader scope. The bottom line is that, while being admittedly non observable, the NN and NNN potentials can be modelled in such a way as to reproduce the available data, and the resulting phenomenological Hamiltonians allow to perform calculations of a variety of nuclear matter properties other than the ground-state energy, whose understanding is needed for a comprehensive description of neutron star structure and dynamics. This line has been pursued by the authors of Refs. [52–56], who carried out pioneering studies of the transport coefficients, the response to neutrino interactions, and the superfluid gap of nuclear matter based on a unified microscopic description of nuclear interactions.

The body of this article is structured as follows. In Sect. II we outline the dynamical model underlying our study, as well as the simple parametrisation adopted to characterise the strength of the repulsive component of the NNN potential. The datasets considered in the analysis are described in Section III, while the results are reported and discussed in Sect. IV. Finally, the summary of our findings and an outlook to future developments can be found in Sect. V. Unless explicitly stated otherwise, we shall use geometric ($G = c = 1$) units.

II. DYNAMICAL MODEL

The model of nuclear dynamics employed in our work is based on a Hamiltonian of the form

$$H = \sum_i \frac{p_i^2}{2m} + \sum_{i < j} v_{ij} + \sum_{i < j < k} V_{ijk}. \quad (1)$$

Here, v_{ij} is the Argonne v_{18} (AV18) nucleon-nucleon (NN) potential [57], corrected to take into account relativistic boost corrections needed to describe NN interactions in the locally inertial frame associated with a star [50, 58]. The NNN potential, V_{ijk} , is assumed to consist of a two-pion exchange contribution, $V_{ijk}^{2\pi}$, and a purely phenomenological repulsive term, V_{ijk}^R which largely determines the stiffness of the nuclear matter EOS at high densities, usually parametrised by the compression modulus K . In the Urbana IX (UIX) model [59], the strengths of $V_{ijk}^{2\pi}$ and V_{ijk}^R are fixed in such a way as to reproduce the ground-state energy of ${}^3\text{H}$ and the saturation density of nuclear matter, respectively. The Hamiltonian comprising the boost-corrected AV18 potential and the UIX potential has been employed to obtain the EOS of Akmal, Pandharipande and Ravenhall (APR) [50], widely used in calculations of neutron star properties. The pressure of isospin-symmetric nuclear matter computed using this Hamiltonian turns out to be consistent with the bounds obtained from the analysis of high-energy nuclear collisions of Ref [19], extending to $\varrho \gtrsim 4\varrho_0$.

In order to explore the possibility to constrain the NNN potential using astrophysical data, we have generated a set of EOSs, computed replacing $V_{ijk}^R \rightarrow \alpha V_{ijk}^R$ and varying the value of the parameter α , which determines the strength of the repulsive NNN interaction. For any values of α , the EOS of charge neutral and β -stable matter consisting of protons, neutrons, electrons and muons has been obtained using a straightforward generalisation of the fitting procedure discussed in Ref. [50] yielding the energy-density functional $\mathcal{H}_\alpha(\varrho, x)$, with x being the proton fraction. Note that, while the EOS of Ref. [50] has been obtained within a variational approach, in our work the contributions arising from $(1 - \alpha)V_{ijk}^R$ are added in perturbation theory. To maintain consistency with the APR EOS, corresponding to $\alpha = 1$, at densities $\varrho \approx \varrho_0$, we have limited our analysis to the range $0.7 \leq \alpha \leq 2$.

Within these bounds the displacement of the equilibrium density with respect to the empirical value remains small, ranging between $\sim 4\%$ and $\sim 20\%$. This range appears to be acceptable, considering that the corresponding change of the energy per particle does not exceed 3%. Moreover, the pressure of isospin-symmetric matter turns out to be compatible with the empirical constraints derived in Ref. [19] for all values of α .

III. ASTROPHYSICAL DATASETS

The EOSs belonging to the family considered in our work only depend on the strength of the NNN force. Therefore, stellar configurations are specified by the values of α and the central pressure p_c , and provide two macroscopic observables: the mass $M(\alpha, p_c)$ and either the radius, $R(\alpha, p_c)$, or the tidal deformability¹, $\Lambda(\alpha, p_c)$, to be compared with observations.

We consider two classes of datasets: (i) the GW observation of the binary NS event² GW170817 [12], and (ii) the spectroscopic observation in the EM bandwidth of the millisecond pulsars PSR J0030+0451 performed by the NICER satellite [8]. Figure 1 shows the confidence intervals in the M - R (a) and Λ_1 - Λ_2 (b) plane for the two datasets considered, together with the results corresponding to stellar configurations having different values of α . It appears that, compared to NICER results, the tidal deformabilities inferred from GW170817 tend to rule out models with $\alpha \gtrsim 1.6$, corresponding to the stiffest EOSs.

To constrain the parameters associated with the EOS, we sample their probability distribution through a Bayesian approach based on Monte Carlo Markov Chain (MCMC) simulations [67]. For a given astrophysical dataset O comprising n observed stars, the probability distribution of $\theta = \{\alpha, p_c^{(i=1, \dots, n)}\}$, is given by

$$\mathcal{P}(\theta|O) \propto \mathcal{P}_0(\theta) \mathcal{L}(O|D(\theta)), \quad (2)$$

where \mathcal{P}_0 is the prior information on θ , and \mathcal{L} is the likelihood function, with $D(\theta)$ being the set of NS observables needed to interpret the data, i.e. the mass, the radius and/or the tidal deformability. For the GW event the likelihood function is given by the marginalised joint

¹ We refer here to the *normalised* tidal deformability $\Lambda = \lambda/M^5$, where $\lambda = 2/3k_2R^5$ is the quadrupolar Love number.

² The LIGO/Virgo collaboration has recently announced the detection of GW190814, an asymmetric binary system featuring a black hole and a $2.6 M_\odot$ companion [60]. While it is still unclear whether the latter is a NS or a black hole, this discovery could have a profound impact on our understanding of stellar evolution, see, e.g., Refs. [61–66].

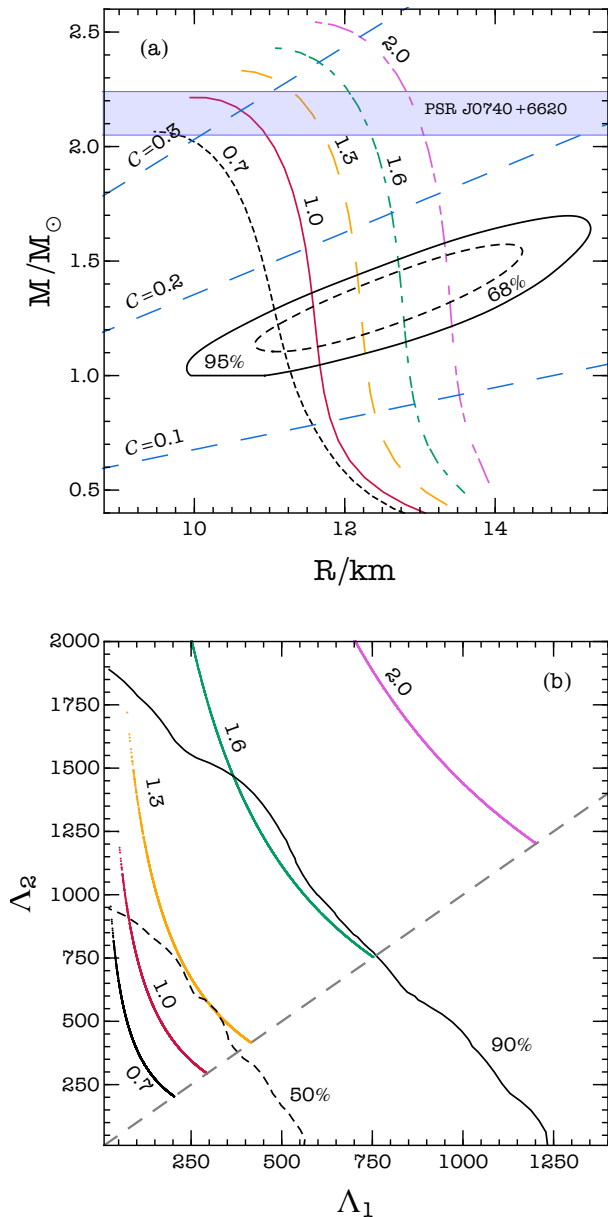


FIG. 1. (a) Mass-radius relations of NS obtained using EOSs corresponding to the values of α specified on top of each curve. The shaded band identifies the most massive pulsar observed so far, PSR J0740+6620 [4]. The closed contours show to the 68% and 95% confidence intervals derived for the NICER pulsar [8]. The dashed straight lines correspond to constant compactness $\mathcal{C} = M/R$. (b) NS models in the Λ_1 - Λ_2 plane for selected values of α , and corresponding to the masses measured for GW170817. The 50% and 90% confidence intervals derived using the GW170817 data [12] are also shown.

density distribution³ inferred by LIGO/Virgo [68]:

$$\mathcal{L}(O_{\text{GW}}|D(\theta)) = \mathcal{L}_{\text{GW}}(M_1, M_2, A_1, A_2). \quad (3)$$

Moreover, given the exquisite precision to which the chirp mass $\mathcal{M} = (M_1 M_2)^{3/5} / (M_1 + M_2)^{1/5}$ of GW170817 has been measured, compared to the individual masses, and following Ref. [37]—see, in particular, the discussion of Appendix B—we fix it to the median value $\mathcal{M} = 1.186 M_\odot$. The mass M_2 , as well as the tidal deformability Λ_2 , is then uniquely determined by M_1 , i.e. by the central density of the primary object, and the number of parameters to be constrained is reduced. Finally, we transform the likelihood function to the mass ratio⁴ $q = M_1/M_2$, and Eq. (2) becomes:

$$\mathcal{P}(\alpha, p_c^{(1)} | O_{\text{GW}}) \propto \mathcal{P}_0(\alpha, p_c^{(1)}, p_c^{(2)}) \mathcal{L}_{\text{GW}}(q, A_1, A_2). \quad (4)$$

Equation (4) shows that the central pressure of the second component of the binary system is also needed. We reconstruct its value by inverting the mass relation $M_2 = M_2(\alpha, p_c^{(2)})$, to lie within the prior support.

For the NICER dataset the likelihood is given by the marginalised joint posterior [69] $\mathcal{L}(O_{\text{em}}|D(\theta)) = \mathcal{L}_{\text{EM}}(M, R)$, such that:

$$\mathcal{P}(\alpha, p_c^{(1)} | O_{\text{EM}}) \propto \mathcal{P}_0(\alpha, p_c^{(1)}) \mathcal{L}_{\text{EM}}(M, R). \quad (5)$$

In the multi-messenger scenario, we consider the joint GW and electromagnetic datasets. Since the two sets of observations are independent, we have

$$\begin{aligned} \mathcal{P}(\alpha, p_c^{(1)}, p_c^{(3)} | O_{\text{GW}}, O_{\text{EM}}) &\propto \mathcal{P}_0(\alpha, p_c^{(1)}, p_c^{(2)}, p_c^{(3)}) \\ &\times \mathcal{L}_{\text{GW}}(q, A_1, A_2) \mathcal{L}_{\text{EM}}(M, R), \end{aligned} \quad (6)$$

where, $p_c^{(1)}$ and $p_c^{(2)}$ refer to the two NSs of GW170817, and the third pressure $p_c^{(3)}$ corresponds to the pulsar observed by NICER.

The values of α are sampled uniformly within the range [0.7, 2], while the central pressures of each star are drawn in the logarithm space between $\ln_{10} p_c \simeq 34.58$ and $\ln_{10} p_c^{\text{max}}(\alpha)$. The latter represents the maximum central pressure for a stable configuration of the EOS family identified by α . The lower end of the prior interval for α is chosen such that the nuclear model supports NSs with masses larger than $1.8 M_\odot$. Moreover, we ask the speed of sound $c_s = \sqrt{dp/d\epsilon}$ inside each stellar configuration to be smaller than the speed of light.

³ The likelihood function can be directly derived from the GW posterior since the joint prior on the masses and the tidal deformabilities is flat. The same holds for the NICER dataset, since the joint prior on the mass and the radius is also flat.

⁴ Changing $\mathcal{L}(M_1, M_2, A_1, A_2) \rightarrow \mathcal{L}(\mathcal{M}, q, A_1, A_2)$ the prior on the chirp mass and the mass ratio, $\mathcal{P}_0(q, \mathcal{M})$, is no longer flat. However, as discussed in [37], reweighting GW170817 so that the prior on the mass ratio and the chirp mass is flat has a negligible effect.

Finally, we also include in the prior information the maximum mass that must be supported by the EOS, provided by the high-precision radio pulsars timing of the binary PSR J0740+6620 [4]. Following the procedure described in [9, 37, 38, 70], we do not impose an hard prior on M_{max} . Rather, we describe the highest mass measurement as a normal distribution $N(\mu, \sigma)$ with mean $\mu = 2.14 M_{\odot}$ and standard deviation $\sigma = 0.09 M_{\odot}$ ⁵. This practically amounts to adding to the MCMC parameter vector an extra central pressure—which we label $p_c^{(M)}$ and corresponds to PSR J0740+6620—and multiplying Eqns. (4), (5) and (6) by the likelihood function $\mathcal{L}_{\text{J0740+6620}} = N(\mu, \sigma)$. For the multimessenger analysis this corresponds to multiply the posterior (6) by $N(\mu, \sigma)$.

We sample the posterior distribution using the *emcee* algorithm with stretch move [71]. For each set of data, we run one hundred walkers of 10^6 samples with a thinning factor of 0.02.

IV. RESULTS AND DISCUSSION

We first consider the constraints inferred from either the EM or the GW observation alone. Panels (a) and (b) of Fig. 2 show the marginalized probability distribution of α inferred for the two datasets, respectively, with and without taking into account the maximum mass bound. Interestingly, the GW data alone do not seem to provide any reliable constraint on α , with the marginal posterior being sharply peaked around the wall at $\alpha = 0.7$ set by the prior. On the other hand, inference from the mass-radius measurements of the millisecond pulsar observed by NICER yields a tighter distribution featuring a peak far from the reference value $\alpha = 1$, and leaves non negligible support for the region outside the prior. The inclusion of the bound provided by PSR J0740+6620 has a strong effect on both observations. This is particular relevant in the case of GW170817, in which $\mathcal{P}(\alpha)$ acquires a well defined shape between $\alpha = 0.8$ and $\alpha = 1.8$. We can identify a 90% confidence interval, which gives around the median $\alpha_{\text{GW}} = 1.25_{-0.53}^{+0.48}$. For the EM observation, inclusion of the maximum mass bound sharpens the posterior and leads to the value $\alpha_{\text{EM}} = 1.52_{-0.47}^{+0.43}$ at 90% probability. Note that NICER points to larger values of α , which is consistent with the fact that, compared to GW170817, the EM measurements seem to favour a stiffer EOS.

The multimessenger scenario, illustrated in panel (c), suggests that, when no additional data is taken into account, the joint NICER–GW inference is dominated by the latter. Including the maximum mass constraint results again in a major change, and leads to $\alpha_{\text{GW+EM}} =$

$1.32_{-0.51}^{+0.48}$ at 90% confidence level. Note that all panels of Fig. 2 show that the requirement that the EOS support the mass of PSR J0740+6620 makes $P(\alpha)$ to have essentially zero support for $\alpha \lesssim 0.8$.

For the sake of completeness, in Fig. 3 we also show the range of variation of the the pressure-energy density relations obtained using the 90% high posterior density intervals of α resulting from our analysis. Considering that the central energy density of the heavier (lighter) NS of GW170817 obtained from our calculations ranges between $6.2 \times 10^{14} \text{g/cm}^3$ and $1.2 \times 10^{15} \text{g/cm}^3$ ($6.7 \times 10^{14} \text{g/cm}^3$ and $1.4 \times 10^{15} \text{g/cm}^3$) for $0.7 \leq \alpha \leq 2.0$, it appears that the EOSs displayed in the figure are largely compatible with the empirical bounds represented by the horizontal lines. Note that the plateau extending between $\sim 1.1 \rho_0$ and $\sim 1.5 \rho_0$ is associated with the transition to a phase featuring neutral pion condensation, discussed in Ref. [50].

V. SUMMARY AND OUTLOOK

The quantity and quality of data provided by the new observatories operating in the GW and EM band have allowed to study the properties of neutron stars evolving in different astrophysical environments. These observations have set multiple and complementary constraints on the NS structure, which have the potential to shed new light on different aspects of the microphysics of dense nuclear matter.

We have investigated the constraints that the recent observations of GW170817 and the NICER pulsar can impose on the potential describing NNN interactions, which are presently unconstrained at densities larger than $\sim \rho_0$. Using a Bayesian approach, we have explored both single and multimessenger constraints, including also the bounds on the maximum mass given by the $2.14 M_{\odot}$ pulsar PSR J0740+6620. For the cases analysed, the results suggest that constraints on the strength α of repulsive NNN interactions are still dominated by the requirement that EOS must support the most massive NS observed. In this regard, the discovery of NSs more massive than PSR J0740+6620 would be potentially able to rule out a large part of the parameter space we sampled, leading to higher values of α , i.e. favouring stiff nuclear matter. The probability distributions inferred for α are compatible with the value $\alpha = 1$, corresponding to the APR EOS [50], providing the baseline for our analysis. However, it is interesting to note that the sampled values of α show large support for $\alpha > 1$, which correspond to more repulsive NNN forces and stiffer EOSs.

The work described in this article should be seen as a first step towards more systematic studies, aimed at obtaining information on microscopic nuclear dynamics from the samples of observed masses, radii and tidal deformabilities.

In principle, chiral effective field theory (EFT) provides

⁵ The actual value of the mass inferred by timing observations is $2.14_{-0.09}^{+0.10} M_{\odot}$. However, the asymmetry of the error has a negligible effect in our analysis

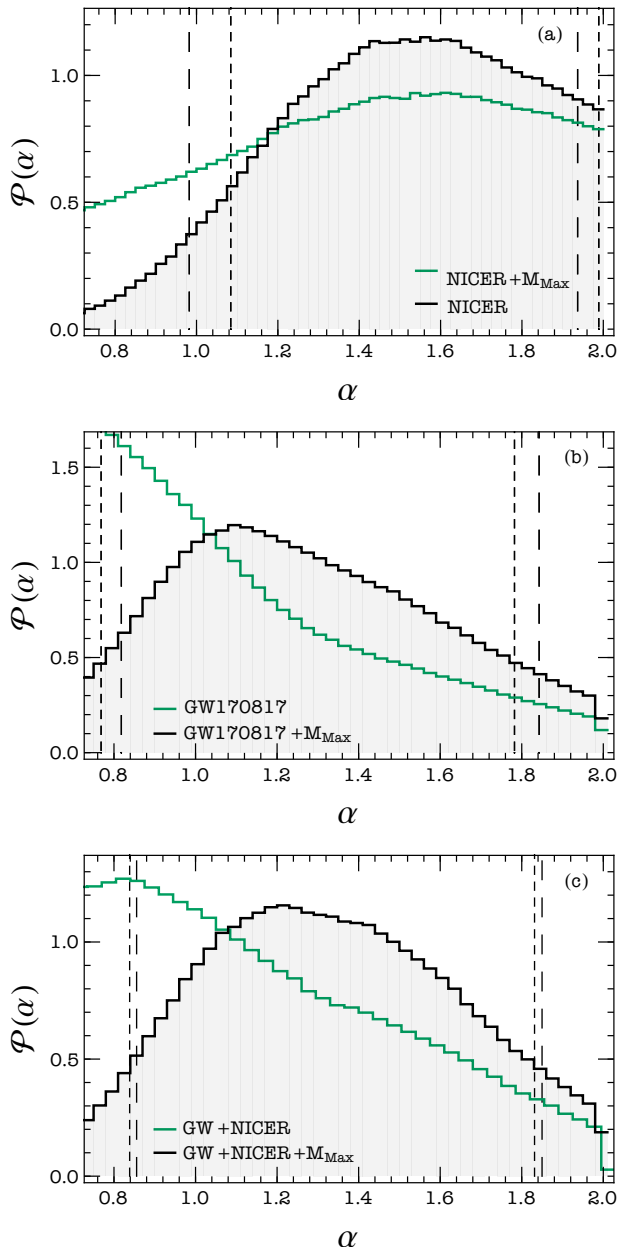


FIG. 2. Posterior probability distribution of the strength of the repulsive three-body potential, α , inferred using the mass radius constraints obtained by NICER for the millisecond pulsar PSR J0030+0451 (a), the GW observation of the binary system GW170817 (b), and combining the two datasets (c). Filled and empty histograms correspond to results obtained including and neglecting the bound on the maximum mass imposed by PSR J0740+6620. Long- and short-dashed vertical lines identify 90% symmetric and highest posterior density intervals, respectively.

a scheme allowing to derive NN and NNN potentials in a fully consistent fashion. However, being obtained from a low-momentum expansion, chiral potentials cannot be used to obtain the EOS of nuclear matter at densities $\rho \gg \rho_0$ [51]. In particular the breakdown scale of EFT

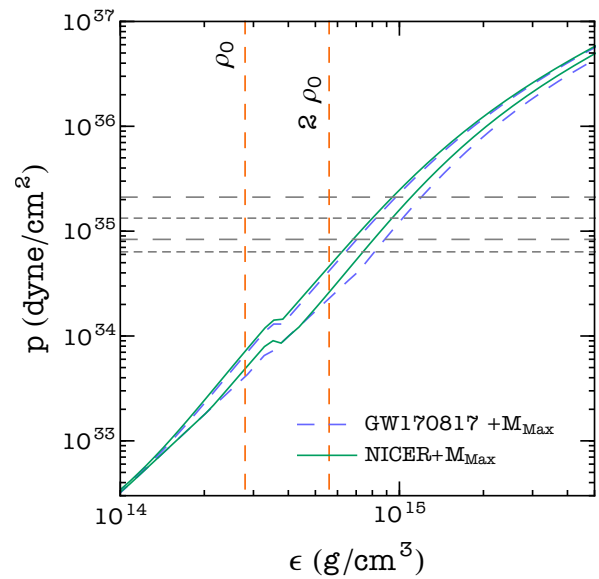


FIG. 3. Range of pressure-energy density relations based on the 90% confidence interval of α inferred using GW170817 and PSR J0030+0451, and including the maximum mass constraint. Horizontal lines identify the 90% high density posterior intervals for the central pressures derived for the heavier (dashed) and lighter (dotted) NS of GW170817.

is expected to be between $1-2\rho_0$. On this respect the authors of [72] explored the possibility of using multi-messenger astronomy to test the predictions of EFT for the EOS only up to $2\rho_0$.

Further applications of the methodology underlying our approach can be pursued following different directions, and in particular considering observations of binary NS by LIGO/Virgo and the Japanese detector KAGRA [73, 74] at design sensitivity, as well as by third generation interferometers, such as the Einstein Telescope [75–77]. In this context, it should be kept in mind that the accuracy of the bounds inferred from GW170817 are expected to improve by at least a factor ~ 3 with LIGO/Virgo at full capacity, and by more than one order of magnitude with the planned Einstein Telescope [78]. The large rate of detections provided by these instruments will allow to stack multiple observations and to study nucleon interactions from constraints on sources within a wider mass spectrum. These data, supplemented by electromagnetic measurements that will also benefit from longer observation times [8], will narrow the bounds on α , with the errors expected to scale as the number of events increases. Finally, the quality and the quantity of data obtained from the new facilities will allow to test more sophisticated models and to explore, for example, the sensitivity of GW and EM signals to an explicit density-dependence of the strength of the three body potential.

ACKNOWLEDGMENTS

The authors are indebted to Valeria Ferrari, Margherita Fasano, and Alessandro Lovato for a crit-

ical reading of this manuscript. This work has been supported by INFN under grant TEONGRAV. A.M. acknowledges support from the Amaldi Research Center, funded by the MIUR program “Dipartimento di Eccellenza”, CUP: B81I18001170001.

-
- [1] P. Demorest, T. Pennucci, S. Ransom, M. Roberts, and J. Hessels, *Nature* **467**, 1081 (2010), arXiv:1010.5788 [astro-ph.HE].
- [2] J. Antoniadis *et al.*, *Science* **340**, 6131 (2013), arXiv:1304.6875 [astro-ph.HE].
- [3] E. Fonseca *et al.*, *Astrophys. J.* **832**, 167 (2016), arXiv:1603.00545 [astro-ph.HE].
- [4] H. T. Cromartie *et al.*, arXiv:1904.06759.
- [5] F. Ozel, G. Baym, and T. Guver, *Phys. Rev. D* **82**, 101301 (2010), arXiv:1002.3153 [astro-ph.HE].
- [6] A. W. Steiner, J. M. Lattimer, and E. F. Brown, *Astrophys. J.* **722**, 33 (2010), arXiv:1005.0811 [astro-ph.HE].
- [7] T. Guver and F. Ozel, *Astrophys. J. Lett.* **765**, L1 (2013), arXiv:1301.0831 [astro-ph.HE].
- [8] T. E. Riley *et al.*, *Astrophys. J. Lett.* **887**, L21 (2019), arXiv:1912.05702 [astro-ph.HE].
- [9] M. Miller *et al.*, *Astrophys. J. Lett.* **887**, L24 (2019), arXiv:1912.05705 [astro-ph.HE].
- [10] B. Abbott *et al.* (LIGO Scientific, Virgo), *Phys. Rev. X* **9**, 011001 (2019), arXiv:1805.11579 [gr-qc].
- [11] B. Abbott *et al.* (LIGO Scientific, Virgo), *Astrophys. J. Lett.* **892**, L3 (2020), arXiv:2001.01761 [astro-ph.HE].
- [12] B. Abbott *et al.* (LIGO Scientific, Virgo), *Phys. Rev. Lett.* **119**, 161101 (2017), arXiv:1710.05832 [gr-qc].
- [13] B.-A. Li and X. Han, *Phys. Lett. B* **727**, 276 (2013).
- [14] P. Russotto *et al.*, *Phys. Rev. C* **94**, 034608 (2016).
- [15] M. B. Tsang *et al.*, *Phys. Rev. Lett.* **102**, 122701 (2009).
- [16] P. Danielewicz and J. Lee, *Nucl. Phys. A* **298**, 1592 (2002).
- [17] B. A. Brown, *Phys. Rev. Lett.* **922**, 1 (2014).
- [18] Z. Zhang and L.-W. Chen, *Phys. Lett. B* **726**, 234 (2013).
- [19] P. Danielewicz, R. Lacey, and W. G. Lynch, *Science* **298**, 1592 (2002).
- [20] S. Shlomo, V. M. Kolomietz, and G. Colò, *The European Physical Journal A - Hadrons and Nuclei* **30**, 23 (2006).
- [21] G. Colò, *Physics of Particles and Nuclei* **39**, 286 (2008).
- [22] T. Hinderer, *Astrophys. J.* **677**, 1216 (2008), arXiv:0711.2420 [astro-ph].
- [23] T. Damour and A. Nagar, *Phys. Rev. D* **80**, 084035 (2009), arXiv:0906.0096 [gr-qc].
- [24] T. Binnington and E. Poisson, *Phys. Rev. D* **80**, 084018 (2009), arXiv:0906.1366 [gr-qc].
- [25] E. E. Flanagan and T. Hinderer, *Phys. Rev. D* **77**, 021502 (2008), arXiv:0709.1915 [astro-ph].
- [26] J. E. Vines and E. E. Flanagan, *Phys. Rev. D* **88**, 024046 (2013), arXiv:1009.4919 [gr-qc].
- [27] J. Vines, E. E. Flanagan, and T. Hinderer, *Phys. Rev. D* **83**, 084051 (2011), arXiv:1101.1673 [gr-qc].
- [28] E. Annala, T. Gorda, A. Kurkela, and A. Vuorinen, *Phys. Rev. Lett.* **120**, 172703 (2018), arXiv:1711.02644 [astro-ph.HE].
- [29] B. Margalit and B. D. Metzger, *Astrophys. J. Lett.* **850**, L19 (2017), arXiv:1710.05938 [astro-ph.HE].
- [30] D. Radice, A. Perego, F. Zappa, and S. Bernuzzi, *Astrophys. J. Lett.* **852**, L29 (2018), arXiv:1711.03647 [astro-ph.HE].
- [31] A. Bauswein, O. Just, H.-T. Janka, and N. Stergioulas, *Astrophys. J. Lett.* **850**, L34 (2017), arXiv:1710.06843 [astro-ph.HE].
- [32] Y. Lim and J. W. Holt, *Phys. Rev. Lett.* **121**, 062701 (2018), arXiv:1803.02803 [nucl-th].
- [33] E. R. Most, L. R. Weih, L. Rezzolla, and J. Schaffner-Bielich, *Phys. Rev. Lett.* **120**, 261103 (2018), arXiv:1803.00549 [gr-qc].
- [34] Z. Carson, A. W. Steiner, and K. Yagi, *Phys. Rev. D* **99**, 043010 (2019), arXiv:1812.08910 [gr-qc].
- [35] S. De, D. Finstad, J. M. Lattimer, D. A. Brown, E. Berger, and C. M. Biwer, *Phys. Rev. Lett.* **121**, 091102 (2018), [Erratum: *Phys. Rev. Lett.* **121**, 259902 (2018)], arXiv:1804.08583 [astro-ph.HE].
- [36] E. Annala, T. Gorda, A. Kurkela, J. Nättilä, and A. Vuorinen, *Nature Phys.* **10**, 1038/s41567-020-0914-9 (2020), arXiv:1903.09121 [astro-ph.HE].
- [37] G. Raaijmakers *et al.*, *Astrophys. J. Lett.* **893**, L21 (2020), arXiv:1912.11031 [astro-ph.HE].
- [38] M. C. Miller, C. Chirenti, and F. K. Lamb, *10.3847/1538-4357/ab4ef9* (2019), arXiv:1904.08907 [astro-ph.HE].
- [39] B. Kumar and P. Landry, *Phys. Rev. D* **99**, 123026 (2019), arXiv:1902.04557 [gr-qc].
- [40] M. Fasano, T. Abdelsalhin, A. Maselli, and V. Ferrari, *Phys. Rev. Lett.* **123**, 141101 (2019), arXiv:1902.05078 [astro-ph.HE].
- [41] H. Güven, K. Bozkurt, E. Khan, and J. Margueron, *Phys. Rev. C* **102**, 015805 (2020), arXiv:2001.10259 [nucl-th].
- [42] S. Traversi, P. Char, and G. Pagliara, *Astrophys. J.* **897**, 165 (2020), arXiv:2002.08951 [astro-ph.HE].
- [43] P. Landry, R. Essick, and K. Chatziioannou, *Phys. Rev. D* **101**, 123007 (2020), arXiv:2003.04880 [astro-ph.HE].
- [44] J. Zimmerman, Z. Carson, K. Schumacher, A. W. Steiner, and K. Yagi, (2020), arXiv:2002.03210 [astro-ph.HE].
- [45] H. O. Silva, A. M. Holgado, A. Cárdenas-Avendaño, and N. Yunes, (2020), arXiv:2004.01253 [gr-qc].
- [46] A. Sabatucci and O. Benhar, *Phys. Rev. C* **1091**, 0545807 (2020).
- [47] L. Baiotti, *Prog. Part. Nucl. Phys.* **109**, 103714 (2019).
- [48] K. Chatziioannou, Neutron star tidal deformability and equation of state constraints, arXiv:2006.03168 [gr-qc] (2020).
- [49] J. Carlson, S. Gandolfi, F. Pederiva, S. C. Pieper, R. Schiavilla, K. E. Schmidt, and R. B. Wiringa, *Rev. Mod. Phys.* **87**, 1067 (2015).
- [50] A. Akmal, V.R. Pandharipande, and D.G. Ravenhall, *Phys. Rev. C* **58**, 1804 (1998).
- [51] O. Benhar, Scale Dependence of Nucleon-Nucleon Potentials, arXiv:1903.11353 [nucl-th] (2019).
- [52] O. Benhar and M. Valli, *Phys. Rev. Lett.* **99**, 232501 (2007).

- [53] O. Benhar, A. Polls, I. Vidaña, and M. Valli, *Phys. Rev. C* **81**, 024305 (2010).
- [54] O. Benhar and N. Farina, *Phys. Lett. B* **680**, 305 (2009).
- [55] A. Lovato, O. Benhar, S. Gandolfi, and C. Losa, *Phys. Rev. C* **89**, 025804 (2014).
- [56] O. Benhar and G. De Rosi, *J. Low. Temp. Phys.* **189**, 250 (2017).
- [57] R. B. Wiringa, V. G. Stoks, and R. Schiavilla, *Phys. Rev. C* **51**, 38 (1995).
- [58] J.L. Forest, V.R. Pandharipande, and J.L. Friar, *Phys. Rev. C* **52**, 568 (1995).
- [59] J. Carlson, V. R. Pandharipande, and R. B. Wiringa, *Nucl. Phys. A* **401**, 59 (1983).
- [60] R. Abbott *et al.* (LIGO Scientific, Virgo), *Astrophys. J.* **896**, L44 (2020), arXiv:2006.12611 [astro-ph.HE].
- [61] E. R. Most, L. J. Papenfort, L. R. Weih, and L. Rezzolla, (2020), arXiv:2006.14601 [astro-ph.HE].
- [62] F. Fattoyev, C. Horowitz, J. Piekarewicz, and B. Reed, (2020), arXiv:2007.03799 [nucl-th].
- [63] S. Clesse and J. Garcia-Bellido, (2020), arXiv:2007.06481 [astro-ph.CO].
- [64] I. Tews, P. T. Pang, T. Dietrich, M. W. Coughlin, S. Antier, M. Bulla, J. Heinzl, and L. Issa, (2020), arXiv:2007.06057 [astro-ph.HE].
- [65] Y. Lim, A. Bhattacharya, J. W. Holt, and D. Pati, (2020), arXiv:2007.06526 [nucl-th].
- [66] B. Biswas, R. Nandi, P. Char, S. Bose, and N. Stergioulas, (2020), arXiv:2010.02090 [astro-ph.HE].
- [67] W. Gilks, S. Richardson, and D. Spiegelhalter, *Markov Chain Monte Carlo in Practice*, Chapman & Hall/CRC Interdisciplinary Statistics (Taylor & Francis, 1995).
- [68] <https://dcc.ligo.org/LIGO-P1800061/public>.
- [69] G. Raaijmakers, S. K. Greif, T. E. Riley, T. Hinderer, K. Hebeler, A. Schwenk, A. L. Watts, S. Nisanke, S. Guillot, J. M. Lattimer, and R. M. Ludlam, 10.5281/zenodo.3711718 (2020).
- [70] D. Alvarez-Castillo, A. Ayriyan, S. Benic, D. Blaschke, H. Grigorian, and S. Typel, *Eur. Phys. J. A* **52**, 69 (2016), arXiv:1603.03457 [nucl-th].
- [71] D. Foreman-Mackey, D. W. Hogg, D. Lang, and J. Goodman, *Publications of the Astronomical Society of the Pacific* **125**, 306–312 (2013).
- [72] R. Essick, I. Tews, P. Landry, S. Reddy, and E. Holz, *Direct Astrophysical Tests of Chiral Effective Field Theory at Supranuclear Densities*, arXiv:2004.07744v3 [astro-ph.HE] (2020).
- [73] K. Somiya (KAGRA), *Class. Quant. Grav.* **29**, 124007 (2012), arXiv:1111.7185 [gr-qc].
- [74] T. Akutsu *et al.* (KAGRA), *Nature Astron.* **3**, 35 (2019), arXiv:1811.08079 [gr-qc].
- [75] M. Maggiore *et al.*, *JCAP* **03**, 050, arXiv:1912.02622 [astro-ph.CO].
- [76] B. S. Sathyaprakash *et al.*, (2019), arXiv:1903.09221 [astro-ph.HE].
- [77] M. Punturo *et al.*, *Class. Quant. Grav.* **27**, 194002 (2010).
- [78] A. Guerra Chaves and T. Hinderer, *J. Phys. G* **46**, 123002 (2019), arXiv:1912.01461 [nucl-th].